

Accepted Manuscript

Double functionalization of a fullerene in drastic arc-discharge conditions: Synthesis and formation mechanism of $C_{2V}(2)-C_{78}Cl_6(C_5Cl_6)$

Cong-li Gao, Laura Abella, Han-Rui Tian, Xin Zhang, Yuan-Yuan Zhong, Yuan-Zhi Tan, Xin-Zhou Wu, Antonio Rodríguez-Forteza, Josep M. Poblet, Su-Yuan Xie, Rong-Bin Huang, Lan-Sun Zheng

PII: S0008-6223(17)31219-8

DOI: [10.1016/j.carbon.2017.11.097](https://doi.org/10.1016/j.carbon.2017.11.097)

Reference: CARBON 12627

To appear in: *Carbon*

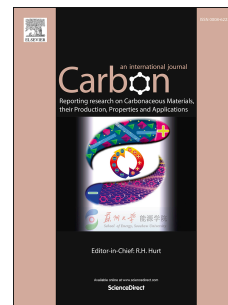
Received Date: 31 August 2017

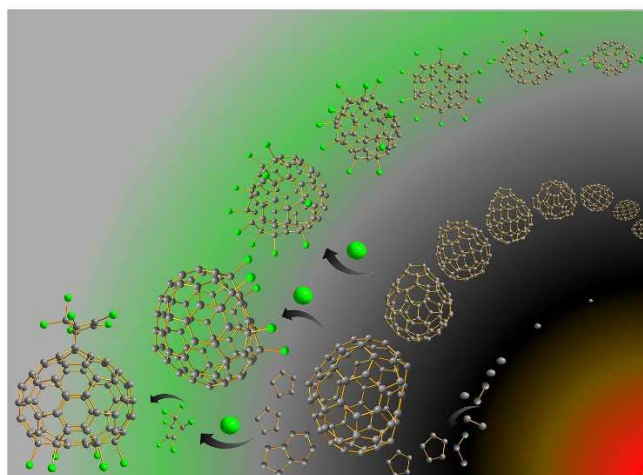
Revised Date: 16 November 2017

Accepted Date: 30 November 2017

Please cite this article as: C.-I. Gao, L. Abella, H.-R. Tian, X. Zhang, Y.-Y. Zhong, Y.-Z. Tan, X.-Z. Wu, A. Rodríguez-Forteza, J.M. Poblet, S.-Y. Xie, R.-B. Huang, L.-S. Zheng, Double functionalization of a fullerene in drastic arc-discharge conditions: Synthesis and formation mechanism of $C_{2V}(2)-C_{78}Cl_6(C_5Cl_6)$, *Carbon* (2018), doi: 10.1016/j.carbon.2017.11.097.

This is a PDF file of an unedited manuscript that has been accepted for publication. As a service to our customers we are providing this early version of the manuscript. The manuscript will undergo copyediting, typesetting, and review of the resulting proof before it is published in its final form. Please note that during the production process errors may be discovered which could affect the content, and all legal disclaimers that apply to the journal pertain.





ACCEPTED MANUSCRIPT

**Double Functionalization of a Fullerene in Drastic Arc-Discharge Conditions:
Synthesis and Formation Mechanism of $C_{2v}(2)-C_{78}Cl_6(C_5Cl_6)$**

Cong-li Gao,^{1 a} Laura Abella,^{1 ab} Han-Rui Tian,^a Xin Zhang,^a Yuan-Yuan Zhong,^a Yuan-Zhi Tan,^a Xin-Zhou Wu,^a Antonio Rodríguez-Fortea,^{* b} Josep M. Poblet,^{* b} Su-Yuan Xie,^{* a} Rong-Bin Huang^a and Lan-Sun Zheng^a

^a *State Key Lab for Physical Chemistry of Solid Surfaces, Collaborative Innovation Center of Chemistry for Energy Materials, Department of Chemistry, College of Chemistry and Chemical Engineering, Xiamen University, Xiamen 361005 (China)*

^b *Departament de Química Física i Inorgànica, Universitat Rovira i Virgili, c/Marcel·lí Domingo 1, 43007 Tarragona (Spain)*

*Corresponding Author.

Tel: (+86) 592-2183047. E-mail: syxie@xmu.edu.c (Su-Yuan Xie),

josepmaria.poblet@urv.cat (Josep M. Poblet), antonio.rodriguez@urv.cat (Antonio Rodríguez-Fortea)

¹ Cong-li Gao and Laura Abella contributed equally.

ABSTRACT

Arc-discharge of graphite is the most prevalent technique for synthesis of novel fullerenes, but the extreme conditions of the carbon arc prevent any currently available instrument from detecting the reaction species inside. To detour the difficulties for probing the derivatization mechanism in the drastic arc-discharge conditions, $C_{78}Cl_6(C_5Cl_6)$ with prototypical $C_{2v}(2)-C_{78}$ cage has been isolated and characterized in the products of the chlorine-involving carbon arc. The structure of $C_{2v}(2)-C_{78}Cl_6(C_5Cl_6)$, featuring with fullerene $C_{2v}(2)-C_{78}$ doubly functionalized by chlorine atoms and perchlorinated cyclopentadiene, has been identified by X-ray crystallography. Confirmed by standard Density Functional Theory (DFT) calculations and Car-Parrinello simulations as well as mass spectrometry, the fullerene core has been revealed to form firstly followed then by reaction with chlorine atoms and afterwards with perchlorinated cyclopentadiene, with implication about stepwise reaction temperatures and sequences for the formation of fullerenes and their derivatives in the otherwise inaccessible extreme conditions of the carbon arc.

1. Introduction

In spite of being rather chaotic and violent, arc-discharge of graphite represents one of the most useful technologies for synthesis of various all-carbon nanostructures such as fullerenes and carbon nanotubes at the present time [1, 2]. Specifically, it is still an irreplaceable technology to synthesize emerging carbon materials, such as graphenes [3], nanotubes of carbon[2] as well as novel exo- or endohedral fullerenes [1,2,4]. The reaction mechanism in the extremely violent conditions of arc-discharge is still a puzzle to chemists due to lack of evidence on intermediates.

Based on ^{13}C -labeling carbon arc reaction pioneers proposed bottom-up mechanism(s) with fullerene growth starting from smaller clusters such as C_2 and C_3 , [5-7] whereas several top-down mechanisms have recently been proposed for understanding the formation of pristine fullerenes or endo-fullerenes in the carbon arc [8,9]. Very recently, several groups have provided new evidences for the bottom-up growth [10-12]. These contradictory statements are symptoms of a long-term puzzle about the mechanism responsible for fullerene formation and derivatization. The difficulties for obtaining the evidence to support the reaction mechanism for carbon cluster growth and derivatization in the arc-discharge of graphite are due to the extremely violent reactions of carbon arc, that prevent currently available technologies from in-situ probing any reactive intermediates. The temperature at the arc center could be higher than $4000\text{ }^\circ\text{C}$ [13], and currently available analytic technologies are unable to directly detect any intermediates in such highly extreme conditions.

As a starting point for further functionalization of fullerene-based materials, a number of prototype fullerene derivatives have been isolated in the soot of carbon arc in the past years [4]. Among them, fullerene chlorides stand out due to their sustainable formation in the chlorine-involving carbon arc and feasible identification by crystallography. Interestingly, the heretofore isolable fullerene chlorides can be exclusively classified into two types, i.e. chlorofullerenes functionalized with chlorine atoms and exo-fullerenes functionalized with chlorinated carbon clusters (CCCs) [4, 14, 15]. Numerous chlorofullerenes, regardless of IPR or non-IPR cages (IPR = isolated pentagon rule[16]), have been produced in the past dozen years[4]. In the presence of CCl_4 , for example, a modified Krätschmer-Huffman arc-discharge has been applied to synthesize smaller non-IPR chlorofullerenes such as D_{5h} -symmetric $^{271}\text{C}_{50}\text{Cl}_{10}$ in 2004[17] and $^{540}\text{C}_{54}\text{Cl}_8$, $^{864}\text{C}_{56}\text{Cl}_{12}$, $^{913}\text{C}_{56}\text{Cl}_{10}$ and $^{916}\text{C}_{56}\text{Cl}_{12}$ later[18-20] (note that the non-IPR fullerenes can be

exclusively specified by Fowler-Manolopoulos chiral code[21]). Larger fullerenes from C₆₀ to C₁₀₈ have been produced as chlorofullerenes in radio-frequency furnace[22] and solvothermal reactions[23,24] as well. For example, in the past years, ^{#916}C₅₆Cl₁₂ [25], ^{#11188}C₇₂Cl₄ [26], and ^{#6094}C₆₈Cl₈ [27], have been synthesized in a radio-frequency furnace starting from graphite in the presence of CCl₄. In addition to chlorofullerenes, a few of exofullerenes functionalized with CCCs were isolated as well [13]. Previous ¹³C-labeling experiments and diffusion-equation calculations suggested that pristine fullerenes grow in a high temperature zone (an arc zone about 2-3 mm from the arc center), whereas smaller CCCs are mainly produced in the region about 30-33 mm from the arc center [13]. Getting insight into the mechanism of exohedral derivatization for both chlorofullerenes and exo-fullerenes in the chlorine-involving arc-discharge of graphite, however, was prevented by the extreme conditions of carbon arc reaction. Therefore, the mechanism responsible for synthetic reaction in the extreme conditions of the chlorine-involving carbon arc is still a “black box” [28].

Unlike the previously produced chlorofullerenes functionalized with chlorine atoms or exofullerenes functionalized with CCCs, in the present contribution, a meaningful C_{2v}(2)-C₇₈Cl₆(C₅Cl₆) *doubly functionalized* with both chlorine atoms and CCCs has been isolated from the products of the chlorine-involving carbon arc. Investigating the unexpected C₇₈Cl₆(C₅Cl₆) by X-ray crystallography, DFT calculations and Car-Parrinello molecular dynamics simulations, we have been able to establish a derivatization mechanism responsible for free-radical addition and 1,4-cycloaddition reaction of C_{2v}(2)-C₇₈ successively with chlorine radicals and C₅Cl₆ and, in turn, make a *qualitative* prediction about the reaction temperatures and sequences for chlorination and exohedral derivatization with CCCs in the arc conditions.

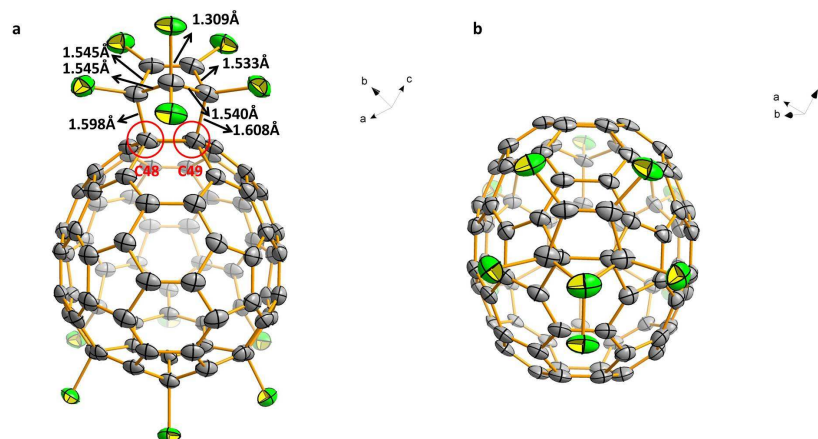


Figure 1. Two views of $C_{2v}(2)-C_{78}Cl_6(C_5Cl_6)$ with 50% thermal ellipsoids. C_{48} and C_{49} atoms, as well as the bond distances involving in the group of C_5Cl_6 are shown.

2. Experimental

2.1 Synthesis

The chlorine-involving arc-discharge was performed in a modified [1] Krätschmer-Huffman arc-discharge device [1,17]. The carbon arc was supplied with the DC power source of 33 V and 100 A, and the reaction atmosphere contained 0.1974 atm He and 0.0395 atm CCl_4 . By ultrasonic extraction with toluene and multistage HPLC separation (detailed separation procedure is described in the Supporting Information), the sample of $C_{2v}(2)-C_{78}Cl_6(C_5Cl_6)$ was purified out of carbon soot. Black crystals of $C_{2v}(2)-C_{78}Cl_6(C_5Cl_6) \cdot 2(C_6H_5Cl)$ suitable for single-crystal X-ray diffraction were obtained by slow evaporation of a solution of $C_{2v}(2)-C_{78}Cl_6(C_5Cl_6)$ in chlorobenzene.

2.2 Identification

The crystallographic data were collected at 100 K on an Agilent SuperNova diffractometer with Cu K α ($\lambda = 1.54184 \text{ \AA}$) micro-focus X-ray source. The data were processed using CrysAlis^{Pro}[29]. The structure was solved and refined using full-matrix least-squares based on F^2 with program SHELXS-2014 and SHELXL-2014[30] within OLEX2[31].

Mass spectra were recorded by a Bruker HCT ion trap instrument interfaced by an atmospheric pressure chemical ionization (APCI) source [32]. In the APCI, ion-molecule reactions occurring at atmospheric pressure were performed to generate the ions, and then the ions were transferred into the mass analyzer by the vacuum interface employed in electrospray ionization [32]. An oven with temperature tunable in the range of 300-550°C was connected to the APCI source for solvent evaporation and possibly sample decomposition.

2.3 DFT calculations

All electronic structure calculations were performed using Density Functional Theory (DFT) methodology with the Amsterdam Density Functional code (ADF2013)[33,34]. The electronic density was provided by the local density approximation using Becke's gradient corrected exchange functional, and Vosko, Wilk, Nusair (VWN) [35] parametrization for correlation, corrected with Perdew's functional (BP86). Triple- ζ polarization basis sets (TZP) were used to describe the electrons of the carbon and chlorine atoms. Scalar relativistic corrections were included by means of the zeroth-order regular approximation (ZORA) formalism [36]. In addition, all the computed structures have also been performed including the Grimme Dispersion D3 method [37].

Molecular dynamics simulations were performed by means of the Car-Parrinello Molecular Dynamics (CPMD¹) program [38]. The description of the electronic structure was based on the expansion of the valence electronic wave functions into a plane wave basis set, which was limited by an energy cutoff of 40 Ry. The interaction between the valence electrons and the ionic cores was treated through the pseudopotential (PP) approximation (Martins-Troullier type) [39]. The functional by Perdew, Burke, and Ernzerhoff (PBE) was selected as the density functional, [40-42] and dispersion corrections (Grimme) were considered. We used a fictitious electron mass of 800 a.u. The simulations were carried out using periodic boundary conditions in a cubic cell with a side length of 15 Å and a time step of 0.144 fs. Even though the size of this cubic cell might seem small to simulate the system in the gas phase, we have checked that it is enough to avoid significant self-interaction between the fullerene and its periodic images (the shortest distance is 4 Å). For the quantitative computation of interaction energies, which is not the case in our qualitative simulations of Cl detachment and attachment processes, the cell size would have to be somewhat larger.

3. Results and discussion

3.1 Geometric structure of $C_{78}Cl_6(C_5Cl_6)$

The parent cage of the doubly functionalized chlorofullerene has been identified by crystallographic measurement as C_{2v} -symmetric IPR-satisfying $C_{2v}(2)-C_{78}$, which could be structurally linked to $D_{3h}(4)-C_{78}$, $D_{3h}(5)-C_{78}$, and $C_{2v}(3)-C_{78}$ by Stone-Wales transformations[43,44]. The two groups, chlorine atoms and perchlorinated cyclopentadiene, are

¹ CPMD. C. M. f. F. S. <http://www.cpmd.org>. Copyright IBM Corp. 1990– 2015.

shown to bind on two different sides of the $C_{2v}(2)$ - C_{78} cage (Fig.1). By free radical addition, the six chlorine atoms in the form of closed chain are respectively bound to the '5, 6, 6' atoms in the coronene motif of the $C_{2v}(2)$ - C_{78} , rendering the sp^2 -hybridized carbon frameworks as an isolated planar aromatic (benzenoid) ring and a curved C_{66} fragment. The pyramidalization angles of the central hexagon in the coronene motif of $C_{2v}(2)$ - C_{78} isomer change from 6.6-6.9° (in the pristine cage) to 1.9-2.4° (in the hexachlorinated cage), showing significant planarization of the benzenoid ring upon chlorination. The perchlorinated cyclopentadiene, which is placed well away from the six chlorine atoms on the coronene plane, has previously been confirmed to be produced together with other perchlorinated polycyclic aromatic hydrocarbons at lower temperature zone away from the arc center [13]. Similar to the Diels-Alder cycloadditions taking place readily on 6,6 pyracylene bond in C_{60} [45], the cycloaddition occurs in a 4, 2 fashion to the 6,6 pyracylene bond of the corresponding cage (C_{48} - C_{49} bond in Fig.1.). The carbon atoms C_{48} and C_{49} are pulled away from the center of the carbon cage toward the addend. The C_{48} - C_{49} distance, 1.559 Å, is substantially elongated if compared to the remaining C-C distances (1.337~1.410 Å) at 6,6 pyracylene bonds.

3.2 Double functionalization with C_5Cl_6 and chlorine

As known, the chamber in our chlorine-involving carbon arc is full of chlorine atoms and C_5Cl_6 units, which are seen to react with C_{60} , C_{70} , and some other carbon clusters [46-50]. Therefore it is likely for either C_5Cl_6 or chlorine atoms to access the pristine C_{78} cage. The singularity in the present case is, however, the double functionalization. To understand the reaction steps that lead to the formation of $C_{2v}(2)$ - $C_{78}Cl_6(C_5Cl_6)$ in the arc-discharge, theoretical analysis regarding two different addition reactions, i.e., Diels-Alder cycloaddition or free radical addition, with both C_5Cl_6 and chlorine atoms was performed (vide infra).

Bond energies (BE) between $C_{2v}(2)-C_{78}$ cage and external groups were analyzed to predict quantitatively the stability of both groups binding to the pristine cage. The C-Cl bond energy per chlorine atom, BE_{C-Cl} , was calculated by equation (1) and the C-(C_5Cl_6) bond energy, $BE_{C-(C_5Cl_6)}$, by equation (2), where x is defined as the number of chlorine atoms.

$$BE_{C-Cl} = (E(C_{78}Cl_x) - E(C_{78}) - x E(Cl))/x \quad (1)$$

$$BE_{C-(C_5Cl_6)} = E(C_{78}Cl_x(C_5Cl_6)) - E(C_{78}Cl_x) - E(C_5Cl_6) \quad (2)$$

Table 1 shows the C-Cl bond energies (BE_{C-Cl}) and the HOMO-LUMO (H-L) gaps for several fullerene derivatives involved in the $C_{2v}(2)-C_{78}Cl_6(C_5Cl_6)$ formation and some other related species [51]. The BE_{C-Cl} are comparable to those computed for other chlorinated fullerenes. For $C_{2v}(2)-C_{78}Cl_2$, with two Cl atoms attached to the coronene motif, the bond energy is $-48.1 \text{ kcal mol}^{-1}$, which is significantly larger (absolute value) than the bond energy for the perchlorinated cyclopentadiene C_5Cl_6 , $-17.1 \text{ kcal mol}^{-1}$. Chlorination of the bond $C_{48}-C_{49}$ where the cycloaddition takes place at C_{48} and C_{49} atoms (Fig.1. and S3) to form $C_{2v}(2)-C_{78}Cl_2^*$ (Table 1), is not so exothermic ($-43.8 \text{ kcal mol}^{-1}$) as chlorination in the coronene motif, but it is still much more favoured than cycloaddition of C_5Cl_6 . Therefore, we conclude that the C-(C_5Cl_6) bond is appreciably much weaker than the C-Cl bond. For $x > 2$, the BE_{C-Cl} become progressively larger as the number of chlorine atoms increases up to $x = 6$ ($-47.6 \text{ kcal mol}^{-1}$). For larger levels of chlorination, as in the experimentally detected $C_{2v}(2)-C_{78}Cl_{18}$ [52] and $C_{2v}(2)-C_{78}Cl_{30}$ [53], a slight drop in BE_{C-Cl} is observed (Table 1).

Although enough chlorine atoms were supplied by CCl_4 , only six chlorine atoms were added to the cage surface, which was merely one third of those in $C_{2v}(2)-C_{78}Cl_{18}$ or one fifth of those in $C_{2v}(2)-C_{78}Cl_{30}$ produced by reaction of $C_{2v}(2)-C_{78}$ with $SbCl_5$ in ampoules at $330-340 \text{ }^\circ\text{C}$ [52,53].

The intermediate compound, $C_{2v}(2)-C_{78}Cl_6$, which is formed before cycloaddition takes place, might be a precursor for chlorination to higher chlorofullerenes such as $C_{2v}(2)-C_{78}Cl_{18}$ [52] and $C_{2v}(2)-C_{78}Cl_{30}$ [53]. Further chlorination to form higher chlorofullerenes might be due to longer reaction time in the previously reported solvothermal reactions[52,53], rather than the limited reaction time in the present arc-discharge process. The hypothesis is supported by the fact that all six chlorine atoms of $C_{2v}(2)-C_{78}Cl_6$ retain their positions in the structure of $C_{2v}(2)-C_{78}Cl_{18}$ and $C_{2v}(2)-C_{78}Cl_{30}$ (Fig. S2a, b and c). Besides, the same pattern is also present in one of the most stable regioisomers of $C_{2v}(2)-C_{78}Cl_8$, as predicted recently by Wang et al[54]. It is not our goal here to compare the stability of this specific chlorination pattern with other regioisomers, but to propose a plausible mechanism for the formation of $C_{2v}(2)-C_{78}Cl_6$, based on successive chlorination steps. In particular, the stepwise chlorination pathway can be understood by the atomic orbital contributions to the HOMOs for $C_{2v}(2)-C_{78}$, $C_{78}Cl_2$ and $C_{78}Cl_4$, as well as the spin density distribution for $C_{78}Cl$, $C_{78}Cl_3$ and $C_{78}Cl_5$ (see Fig S3 and Fig. S4 and Table S1). Carbon atoms of $C_{2v}(2)-C_{78}$ that possess the largest contributions to HOMO are shown in grey circles in Fig. S3. These carbon atoms represent the reactive sites of the prototypical fullerene and are those firstly bonded by chlorine atoms. On the other hand, the carbon atoms where C_5Cl_6 is added, i.e. C_{48} and C_{49} (see Fig.1. or Fig. S3.) present insignificant contributions to the HOMO in line with the fact that chlorine atoms are added first to the coronene motif.

Table 1. C-Cl bond energies (BE_{C-Cl}) and HOMO-LUMO (H-L) gaps for different systems related to $C_{2v}(2)-C_{78}Cl_6(C_5Cl_6)$ formation, and for experimentally detected $C_{2v}(2)-C_{78}Cl_{18}$ and $C_{2v}(2)-C_{78}Cl_{30}$.^{a)}

System	BE_{C-Cl}	H-L gap ^{b)}
$C_{2v}(2)-C_{78}$		1.064
$C_{2v}(2)-C_{78}Cl$	-33.1	
$C_{2v}(2)-C_{78}Cl_2$	-43.0	1.059
$C_{2v}(2)-C_{78}Cl_2^c)$	-38.7	1.187
$C_{2v}(2)-C_{78}Cl_3$	-41.7	
$C_{2v}(2)-C_{78}Cl_4$	-45.4	1.058
$C_{2v}(2)-C_{78}Cl_5$	-44.8	
$C_{2v}(2)-C_{78}Cl_6$	-47.6	1.167
$C_{2v}(2)-C_{78}Cl_{18}$	-45.4	2.373
$C_{2v}(2)-C_{78}Cl_{30}$	-43.8	2.575

a) BE_{C-Cl} in kcal mol^{-1} and H-L gaps in eV; b) H-L gaps only for closed-shell systems; c) The Cl atoms are not bonded to the coronene motif, but to C_{48} and C_{49} atoms where otherwise cycloaddition takes place as shown in Fig.1.

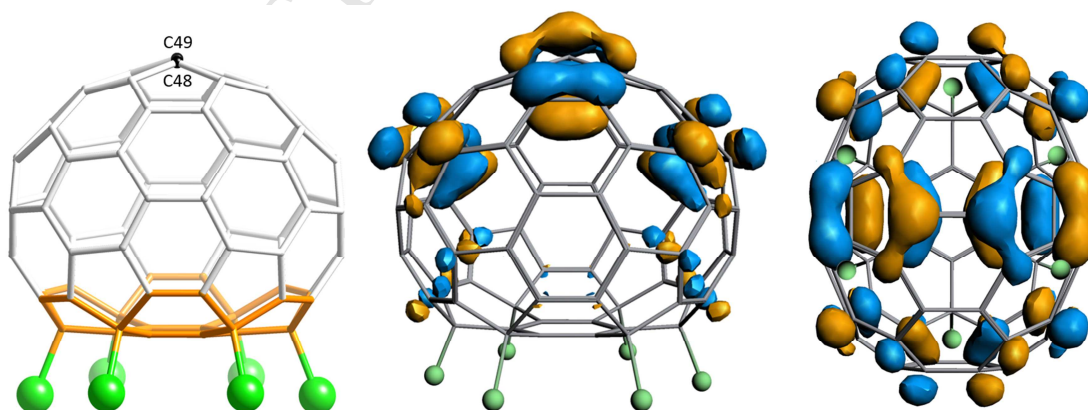


Figure 2. Representation of $C_{2v}(2)-C_{78}Cl_6$ (left) and its LUMO (middle). The right one is the top view of the LUMO showing the 48-49 bond presenting the largest contributions with the appropriate phase (antibonding) to interact with the HOMO of the diene C_5Cl_6 .

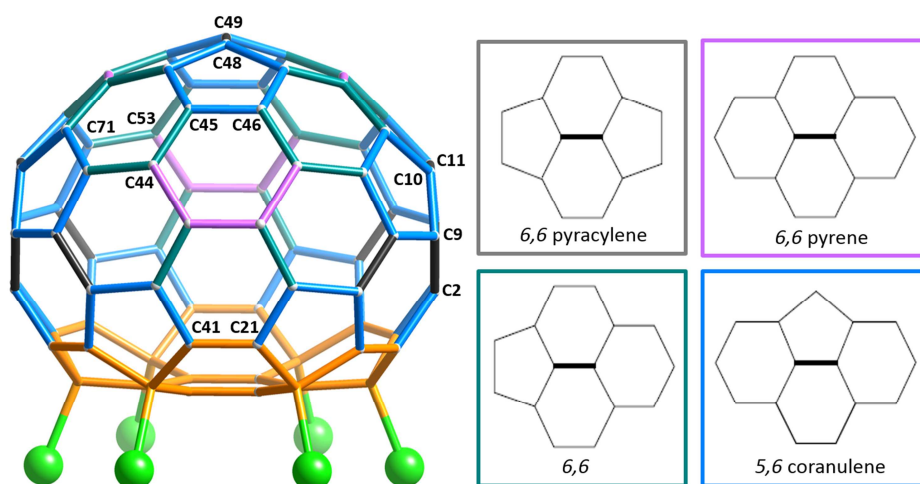


Fig. 3. Structure and types of C-C bonds for $C_{2v}(2)-C_{78}Cl_6$. In the structure, each bond is coloured according to its type. Grey for the 6,6 pyracylene bond, pink for the 6,6 pyrene bond, green for the other 6,6 bond, and blue for the 6,6 corannulene bond. Coronene motif is highlighted in orange. Carbon atoms labelled in Table 2 are also represented in the structure.

The last step in the reaction mechanism to obtain $C_{2v}(2)-C_{78}Cl_6(C_5Cl_6)$ was characterized to be a Diels-Alder reaction. In the last twenty years, numerous experimental [55,56] and theoretical studies about Diels-Alder reaction in C_{60} and C_{70} cages [57-59] as well as in endohedral metallofullerenes [60,61] have been reported, principally because fullerenes possess a reactive dienophile character derived from their electron-deficient properties. The addition pattern of the Diels-Alder reaction can be understood by the Woodward-Hoffmann rules [62] and

the Frontier Molecular Orbital theory [63, 64], when kinetically controlled. In this context, the $C_{2v}(2)-C_{78}Cl_6$ acts as a dienophile and its LUMO is expected to play a key role in the interaction with the HOMO of C_5Cl_6 , which acts as a diene. Addition sites are selected from those atoms that show large orbital contribution to the LUMO. The shape of the LUMO for $C_{2v}(2)-C_{78}Cl_6$ is represented in Fig.2. The largest contribution to the LUMO is found for C_{48} and C_{49} , i.e. those carbon atoms where C_5Cl_6 is experimentally bonded. Thus, this simple qualitative theory predicts that the Diels-Alder reaction occurs on a 6,6 pyracylene bond, in good agreement with the present experiment and with other experimental and computational studies previously published[65].

To gain more insight into the reactivity of the system and to check whether adduct on bond 48-49 is also one of the thermodynamic products, other bonds for the Diels-Alder reaction between C_5Cl_6 and $C_{2v}(2)-C_{78}Cl_6$ cage have also been analyzed. $C_{2v}(2)-C_{78}$ has four types of C-C bonds, namely, the so-called 6,6, 6,6-pyracylene, 6,6-pyrene and 5,6-corannulene bonds (see Fig. 3). All of them have different reactivity, which can be rationalized by their different bond distances and pyramidalization angles, as shown in Table 2. The lowest-energy adducts are those formed on three pyracylene bonds (10-11, 2-9 and 48-49), which are essentially degenerate. The pyracylene bonds show, in general, the lowest C-C distances (higher double bond character) and among the highest pyramidalization angles (lower deformation energies), see Table 2, which make them more reactive to diene attack than other bonds, as observed for other fullerenes[60,61]. Among them, adduct on bond 48-49 show the largest HOMO-LUMO gap (1.541 eV). Interestingly, adduct on pyracylene bond 21-41 shows significantly higher energy than the others. Two reasons are behind such a different behavior: a lower pyramidalization angle due to its position next to the coronene motif (see Fig. 3) and a much higher steric

hindrance between the chlorine atoms and the C_5Cl_6 group. Adducts on other 6,6 and 5,6 bonds are much higher in energy as well.

Table 2

Relative energies (E_{rel}), HOMO-LUMO (H-L) gaps, C-(C_5Cl_6) bond energies (BE), C-C bond distances, pyramidalization angles and types of bonds for different sites of C_5Cl_6 addition on the $C_{2v}(2)-C_{78}Cl_6$ cage.^{a)}

Bond	E_{rel}	H-L gap	BE	C-C reactant ^{b)}	C-C product ^{b)}	pyr angle ^{c)}	Type of bond
48-49	0.2	1.541	-17.2	1.380	1.571	11.1	6,6 pyracylene
44-45	16.2	1.191	-1.3	1.412	1.609	8.8	6,6
45-46	24.0	0.735	6.6	1.453	1.606	9.7	5,6 corannulene
10-11	0.0	1.350	-17.4	1.389	1.589	11.5	6,6 pyracylene
2-9	0.1	1.071	-17.3	1.405	1.630	11.8	6,6 pyracylene
53-71	17.4	0.860	0.0	1.428	1.638	9.1	6,6
27-28	30.8	1.192	13.3	1.464	1.733	8.8	6,6 pyrene
21-41	28.7	0.966	11.2	1.360	1.566	9.1	6,6 pyracylene

a) E_{rel} and BE in kcal mol^{-1} , H-L gaps in eV, bond distances in Å and pyramidalization angles in degrees.

b) Computed bond distances on $C_{2v}(2)-C_{78}Cl_6$ and $C_{2v}(2)-C_{78}Cl_6(C_5Cl_6)$.

c) Average pyramidalization angles of the two atoms that constitute the bond.

3.3 Stability of both C_5Cl_6 and chlorine groups in $C_{78}Cl_6(C_5Cl_6)$

Car-Parrinello molecular dynamics simulations were also performed to provide more insight into the stability of both groups found in $C_{2v}(2)-C_{78}Cl_6(C_5Cl_6)$. Trajectories for $C_{2v}(2)-C_{78}Cl_6$, $C_{2v}(2)-C_{78}(C_5Cl_6)$ and $C_{2v}(2)-C_{78}Cl_6(C_5Cl_6)$ were analyzed at different temperatures. For example, motion of chlorine atoms of $C_{2v}(2)-C_{78}Cl_6$ at high temperature (1500 K) is shown in Fig. S5. Chlorine atoms remain in their original positions during the short time of simulation (19 ps). Besides, simulations for $C_{2v}(2)-C_{78}(C_5Cl_6)$ done at different temperatures (300, 800 and 1000 K), show that C_5Cl_6 only remains on the cage at 300 K in the rather short time scale simulated here (around 15 ps). Trajectories at higher temperatures, 800 and 1000 K, show that the organic group is lost after 7 and 3 ps, respectively. Finally, molecular dynamics simulations for $C_{2v}(2)-C_{78}Cl_6(C_5Cl_6)$ at high temperatures (800, 1000 and 1500 K) indicated that the C_5Cl_6 group is lost before chlorine atoms after short time (4, 1 and less than 1 ps, respectively). It is also observed that the C_5Cl_6 group in $C_{2v}(2)-C_{78}Cl_6(C_5Cl_6)$ leaves faster than in $C_{2v}(2)-C_{78}(C_5Cl_6)$.

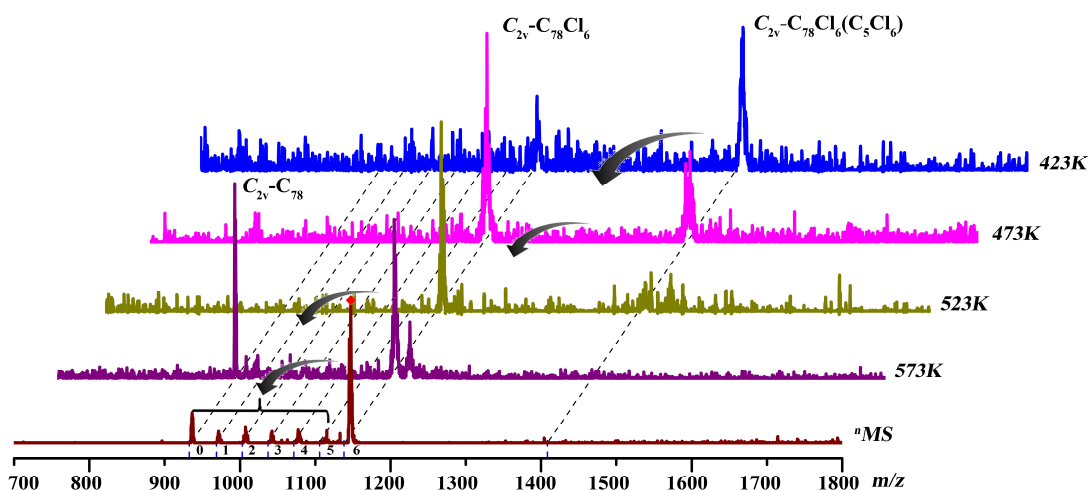


Fig. 4. Mass spectra of $C_{2v}(2)-C_{78}Cl_6(C_5Cl_6)$ obtained at different ionization temperatures and multi-stage mass spectrum (nMS) for the fragment ions of $C_{2v}(2)-C_{78}Cl_6$ at 523 K.

Stepwise mass spectra of $C_{2v}(2)-C_{78}Cl_6(C_5Cl_6)$ were recorded at different ionization temperatures to confirm the Car-Parrinello MD results. As shown in Fig. 4, mass peaks at m/z 936 and 1149 respectively corresponding to C_{78} and $C_{78}Cl_6$ dominantly appeared when the vaporization/ionization temperature was 573 K. A single and strong peak at m/z 1149 occurred when the temperature was 523 K. Only when the temperatures drop to 423 K, the mother peak at m/z 1419 corresponding to $C_{78}Cl_6(C_5Cl_6)$ gradually dominated the mass spectrum. Six fragment ions of $C_{78}Cl_x$ ($x=0-5$) were simultaneously observed in the multi-stage mass spectrum for fragmentation of $C_{2v}(2)-C_{78}Cl_6$ at 523 K. Likely it was difficult for the other five chlorine atoms to remain on the coronene motif, once any chlorine atom left from the cage. The six chlorine atoms leave from carbon cage $C_{2v}(2)-C_{78}$ concurrently, probably due to breakage of the aromatic (benzenoid) ring isolated by the six chlorines. It is worth remarking here that the mass spectra are in good agreement with the Car-Parrinello MD simulations and the computations on bond energies about the C-(C_5Cl_6) bond weaker than C-Cl bond. Therefore, it can be concluded from both theoretical and experimental aspects that C_5Cl_6 is lost before Cl atoms at high temperature.

3.4 Formation of $C_{78}Cl_6(C_5Cl_6)$ in the chlorine-involving carbon arc

In a typical chlorine-involving arc-discharge, amounts of carbon atoms, reactive small carbon clusters with free radicals, unstable fullerene intermediates, chlorine atoms, CCCs, and fullerene chlorides are simultaneously coexisting. In principle, diverse species could be produced at different venues during the arc-discharge process. In our previous ^{13}C -labeling experiments and diffusion-equation calculations, it has been suggested that pristine fullerenes grow at a high

temperature zone (an arc zone about 2-3 mm from the arc center), independent of chlorine, and the CCCs can form in the region about 30-33 mm from the arc center [13]. Thus, we predict that, fullerenes with fused pentagons or heptagon can be in situ synthesized in the forms of chlorinated fullerenes by reaction with chlorine atoms at a relative low temperature zone. For the formation of these chlorinated fullerenes, aromaticity[66,67], cage strain[69], and steric hindrance[69] from adjacent chlorine atoms as well as other factors[68,69], such as the structural motifs[68-71] in the final fullerene derivatives, all play important roles. We have been able to predict the relative stability of chlorinated fullerenes based on these principles. Different from all of previously isolatable fullerene derivatives that can be classified into two catalogues, i.e., chlorofullerenes and exo-fullerenes functionalized with perchlorinated carbon clusters[14, 15, 18-20, 22-27], the fullerene derivative of $C_{2v}(2)-C_{78}Cl_6(C_5Cl_6)$ functionalized with both chlorine atoms and CCCs affords a precious structure to probe the venue for fullerene derivatization in the chaotic conditions of carbon arc. The synthesis of $C_{2v}(2)-C_{78}Cl_6(C_5Cl_6)$ can be seen just like a travel of $C_{2v}(2)-C_{78}$ in the complex arc-discharge system from the high temperature central zone to the low temperature peripheral zone. Therefore, the formation of $C_{2v}(2)-C_{78}Cl_6(C_5Cl_6)$ is proposed to take place in three steps, in which firstly the carbon cage is formed at very high temperatures in a zone very close to the arc center, then six Cl atoms are attached to the coronene motif of $C_{2v}(2)-C_{78}$ in a zone still nearby the arc center but at lower temperatures, and later C_5Cl_6 is added to the corresponding $C_{48}-C_{49}$ bond further from the center at a *much lower* temperature. Briefly, the fullerene $C_{2v}(2)-C_{78}$ is formed at a higher temperature, and chlorine atoms and CCCs exist at a lower temperature and do not participate in the formation of the fullerenes at higher temperature zone. The chlorine atoms access the cage at a lower temperature after the bare

fullerene grows at a higher temperature (c.f. >2000 K) [72], and then the chlorofullerene arrives at an even lower temperature zone and reacts with CCCs such as C_5Cl_6 .

4. Conclusion

In conclusion, the $C_{78}Cl_6(C_5Cl_6)$ with prototypical $C_{2v}(2)-C_{78}$ cage doubly functionalized by both chlorine atoms and perchlorinated cyclopentadiene has been trapped and isolated in the products of a chlorine-involving Krätschmer-Huffman arc-discharge. The structure of the prototypical fullerene derivatives, accurately determined by single-crystal X-ray diffraction, can reflect the reaction venue for the fullerene derivatization in the arc-discharge of graphite. Taking into account that C- C_5Cl_6 bond is weaker than C-Cl bond, the former shows lower bond energy and leaves earlier than the six chlorine atoms at high temperature based on Car-Parrinello MD simulations. Results from computations are also in accord with the mass spectra of $C_{2v}(2)-C_{78}Cl_6(C_5Cl_6)$ at different ionization temperatures. The stepwise chlorination pathway in coronene motif of $C_{2v}(2)-C_{78}$ can be rationalized by free radical addition considering the HOMO and the spin density distributions of the pristine cage and the intermediates. On the other hand, a Diels-Alder reaction between $C_{2v}(2)-C_{78}Cl_6$ and C_5Cl_6 can also be explained by simple qualitative MO arguments. Accordingly, the formation mechanism for $C_{2v}(2)-C_{78}Cl_6(C_5Cl_6)$ has been elucidated that the nascent $C_{2v}(2)-C_{78}$ reacts first with chlorine atoms by free radical addition and then with perchlorinated cyclopentadiene by 1,4-cycloaddition. This work provides a new concept about the multifunctional fullerene derivatives in-situ captured in the carbon arc being a detector to probe the otherwise inaccessible extreme reactions.

Appendix A. Supplementary data.

Supplementary data related to this article can be found at...

Acknowledgements

This work was supported by the 973 Project (2014CB845601) and the National Science Foundation of China (U1205111, 21390390). This work was also supported by the Spanish Ministerio de Ciencia e Innovación (Project No. CTQ2014-52774-P) and by the Generalitat de Catalunya (2014SGR-199 and XRQTC). J.M.P thanks the ICREA foundation for an ICREA ACADEMIA award. L.A. thanks the Generalitat de Catalunya for a predoctoral fellowship (FI-DGR 2014) and also the Chinese Government for a scholarship to study in China (Bilateral Program 2015-1016).

References

- [1] Krätschmer W, Lamb L. D, Fostiropoulos K, Huffman D. R. Solid C₆₀: A New Form of Carbon. *Nature* 1990; 347: 354–8.
- [2] Iijima S. Helical Microtubules of Graphitic Carbon. *Nature* 1991; 354: 56–8.
- [3] Wu Y, Wang B, Ma Y, Huang Y, Li N, Zhang F, et al. Efficient and Large-Scale Synthesis of Few-Layered Graphene Using an Arc-Discharge Method and Conductivity Studies of the Resulting Films. *Nano Res.* 2010; 3(9): 661–9.
- [4] Tan Y.-Z, Xie S.-Y, Huang R.-B, Zheng L.-S. The Stabilization of Fused-Pentagon Fullerene Molecules. *Nat. Chem.* 2009; 1: 450–60.
- [5] Meijer G, Bethune D. S. Laser Deposition of Carbon Clusters on Surfaces: A New Approach to the Study of Fullerenes. *J. Chem. Phys.* 1990; 93(11): 7800–2.

- [6] Hawkins J. M, Meyer A, Loren S, Nunlis, R. Statistical Incorporation of Carbon-13 $^{13}\text{C}_2$ Units into C_{60} (Buckminsterfullerene). *J. Am. Chem. Soc.* 1991; 113(24): 9394–5.
- [7] Dunk P. W, Kaiser N. K, Hendrickson C. L, Quinn J. P, Ewels C. P, Nakanishi Y, et al. Closed Network Growth of Fullerenes. *Nat. Commun.* 2012; 3: 855.
- [8] Irle S, Zheng G, Wang Z, Morokuma K. The C_{60} Formation Puzzle “Solved”: QM/MD Simulations Reveal the Shrinking Hot Giant Road of the Dynamic Fullerene Self-Assembly Mechanism. *J. Phys. Chem. B* 2006; 110(30): 14531–45.
- [9] Zhang J, Bowles F. L, Bearden D. W, Ray W. K, Fuhrer T, Ye Y, et al. A Missing Link in the Transformation from Asymmetric to Symmetric Metallofullerene Cages Implies a Top-down Fullerene Formation Mechanism. *Nat. Chem.* 2013; 5: 880–5.
- [10] Dunk P. W, Mulet-Gas M, Nakanishi Y, Kaiser N. K, Rodríguez-Forteza A, Shinohara H, et al. Bottom-up Formation of Endohedral Mono-Metallofullerenes Is Directed by Charge Transfer. *Nat. Commun.* 2014; 5 (22): 5844.
- [11] Mulet-Gas M, Abella L, Ceron M.R, Castro E, Marshall A.G, Rodriguez-Forteza A, Echegoyen L, Poblet J.M, Dunk P.W, Transformation of Doped Graphite into Cluster-encapsulated Fullerene Cages, *Nat. Commun.* 2017; 8: 1222.
- [12] Chen C.-H, Abella L, Cerón M. R, Guerrero-Ayala M. A, Rodríguez-Forteza A, Olmstead M. M, et al. Zigzag Sc_2C_2 Carbide Cluster inside a [88] Fullerene Cage with One Heptagon, $\text{Sc}_2\text{C}_2@C_{88}(\text{Hept})-C_{88}$: A Kinetically Trapped Fullerene Formed by C_2 Insertion? *J. Am. Chem. Soc.* 2016; 138 (39): 13030–7.

- [13] Tan Y.-Z, Chen R.-T, Liao Z.-J, Li J, Zhu F, Lu X, et al. Carbon Arc Production of Heptagon-Containing fullerene[68]. *Nat. Commun.* 2011; 2: 420.
- [14] Troyanov S. I, Popov A. A. A [70] Fullerene Chloride, $C_{70}Cl_{16}$, Obtained by the Attempted Bromination of C_{70} in $TiCl_4$. *Angew. Chem. Int. Ed.* 2005; 44(27): 4215–8.
- [15] Mueller A, Ziegler K, Amsharov K. Y, Jansen M. Perchloropyracylene and Its Fusion with C_{60} by Chlorine-Assisted Radio-Frequency Furnace Synthesis. *Chem. Eur. J.* 2011; 17(42): 11797–804.
- [16] Kroto H. W. The Stability of the Fullerenes C_n , with $N = 24, 28, 32, 36, 50, 60$ and 70. *Nature* 1987; 329: 529–31.
- [17] Xie S.-Y. Capturing the Labile Fullerene[50] as $C_{50}Cl_{10}$. *Science* 2004; 304(5671): 699.
- [18] Tan Y.-Z, Li J, Zhu F, Han X, Jiang W.-S, Huang R.-B, et al. Chlorofullerenes Featuring Triple Sequentially Fused Pentagons. *Nat. Chem.* 2010; 2: 269–73.
- [19] Tan Y.-Z, Han X, Wu X, Meng Y.-Y, Zhu F, Qian Z.-Z, et al. An Entrant of Smaller Fullerene: C_{56} Captured by Chlorines and Aligned in Linear Chains. *J. Am. Chem. Soc.* 2008; 130(46): 15240–1.
- [20] Zhou T, Tan Y.-Z, Shan G.-J, Zou X.-M, Gao C.-L, Li X, et al. Retrieving the Most Prevalent Small Fullerene C_{56} . *Chem. Eur. J.* 2011; 17(31): 8529–32.
- [21] Fowler P. W, Manolopoulos D. E. *An atlas of fullerenes*, Oxford Univ. Press, 1995.
- [22] Mueller A, Ziegler K, Amsharov K. Y, Jansen M. In Situ Synthesis of Chlorinated Fullerenes by the High-Frequency Furnace Method. *Eur. J. Inorg. Chem.* 2011; 2011(2):

268–72.

- [23] Troshin P. A, Lyubovskaya R. N, Ioffe I. N, Shustova N. B, Kemnitz E, Troyanov S. I. Synthesis and Structure of the Highly Chlorinated [60]Fullerene $C_{60}Cl_{30}$ with a Drum-Shaped Carbon Cage. *Angew. Chem. Int. Ed.* 2005; 44(2): 234–7.
- [24] Wang S, Yang S, Kemnitz E, Troyanov S. I. New Giant Fullerenes Identified as Chloro Derivatives: Isolated-Pentagon-Rule $C_{108}(1771)Cl_{12}$ and $C_{106}(1155)Cl_{24}$ as Well as Nonclassical $C_{104}Cl_{24}$. *Inorg. Chem.* 2016; 55(12): 5741–3.
- [25] Ziegler K, Mueller A, Amsharov K. Y, Jansen M. Capturing the Most-Stable C_{56} Fullerene Cage by In Situ Chlorination. *Chem. Asian J.* 2011; 6(9): 2412–8.
- [26] Ziegler K, Mueller A, Amsharov K. Y, Jansen M. Disclosure of the Elusive C_{2v} - C_{72} Carbon Cage. *J. Am. Chem. Soc.* 2010; 132(48): 17099–101.
- [27] Amsharov K. Y, Ziegler K, Mueller A, Jansen M. Capturing the Antiaromatic $^{6094}C_{68}$ Carbon Cage in the Radio-Frequency Furnace. *Chem. Eur. J.* 2012; 18(30): 9289–93.
- [28] Deng S. L, Xie S.Y, Huang R.B, Zheng L. S. The Formation Mechanism of Fullerene. *Sci. China Chem.*, 2012; 42: 1587-97.
- [29] Agilent Technologies Inc., Santa Clara, CA, USA, 2011.
- [30] Sheldrick G. M. A Short History of SHELX. *Acta Crystallogr. A.* 2008; 64: 112–22.
- [31] Dolomanov O. V, Bourhis L. J, Gildea R. J, Howard J. A. K, Puschmann H. OLEX2 : A Complete Structure Solution, Refinement and Analysis Program. *J. Appl. Crystallogr.* 2009; 42: 339–41.

- [32] Gross J. H. *Mass Spectrometry: A Textbook*; 2 ed, Springer Link: Verlag: Berlin, Germany, 2004: 465-6.
- [33] Baerends E. J, Ellis D. E, Ros P. ADF2013.01. Department of Theoretical Chemistry, Vrije Universiteit: Amsterdam; 2013.
- [34] Te Velde G, Bickelhaupt F. M, Baerends E. J, Fonseca Guerra C, van Gisbergen S. J. A, Snijders J. G, et al. *Chemistry with ADF*. *J. Comput. Chem.* 2001; 22(9): 931–67.
- [35] Vosko S. H, Wilk L, Nusair M. *Accurate Spin-Dependent Electron Liquid Correlation Energies for Local Spin Density Calculations: A Critical Analysis*. *Can. J. Phys.* 1980; 58(8): 1200–11.
- [36] Becke A. D. *Density - functional Thermochemistry. III. The Role of Exact Exchange*. *J. Chem. Phys.* 1993; 98: 5648–52.
- [37] Grimme S. *Semiempirical GGA-Type Density Functional Constructed with a Long-Range Dispersion Correction*. *J. Comput. Chem.* 2006; 27(15): 1787–99.
- [38] Car R, Parrinello M. *Unified Approach for Molecular Dynamics and Density-Functional Theory*. *Phys. Rev. Lett.* 1985; 55(22-25): 2471–4.
- [39] Troullier N, Martins J. L. *Efficient Pseudopotentials for Plane-Wave Calculations*. *Phys. Rev. B* 1991; 43(3-15): 1993–2006.
- [40] Perdew J. P, Burke K, Ernzerhof M. *Generalized Gradient Approximation Made Simple*. *Phys. Rev. Lett.* 1996; 77(18-28): 3865–8.

- [41] Hirsch A, Brettreich M. Fullerenes: Chemistry and Reactions; Wiley-VCH, 2005.
- [42] Álvarez-Moreno M, de Graaf C, López N, Maseras F, Poblet J. M, et al. Managing the Computational Chemistry Big Data Problem: The ioChem-BD Platform. *J. Chem. Inf. Model.* 2015; 55(1): 95–103.
- [43] Stone A. J, Wales D. J. Theoretical Studies of Icosahedral C_{60} and Some Related Species. *Chem. Phys. Lett.* 1986; 128(5-6): 501–3.
- [44] Diederich F, Whetten R. L, Thilgen C, Ettl R, Chao I, Alvarez M. M. Fullerene Isomerism: Isolation of C_{2v} - C_{78} and D_3 - C_{78} . *Science* 1991; 254(5039): 1768–70.
- [45] Lamparth I, Maichle–Mössmer C, Hirsch A. Reversible Template-Directed Activation of Equatorial Double Bonds of the Fullerene Framework: Regioselective Direct Synthesis, Crystal Structure, and Aromatic Properties of T_h - $C_{66}(\text{COOEt})_{12}$. *Angew. Chem. Int. Ed.* 1995; 34(15): 1607–9.
- [46] Rotello V. M, Howard J. B, Yadav T, Conn M.M, Viani E, Giovane L M, Lafleur A L, Isolation of Fullerene Products from Flames: Structure and Synthesis of the C_{60} -cyclopentadiene adduct. *Tetrahedron Lett.* 1993; 34(10): 1561-1562.
- [47] Xie S. Y, Huang R. B, Deng S. L, Yu L. J, Zheng L. S, Synthesis, Separation, and Characterization of Fullerenes and Their Chlorinated Fragments in the Glow Discharge Reaction of Chloroform. *J. Phys. Chem. B* 2001; 105(9): 1734-1738.
- [48] Xie S. Y, Deng S. L, Yu L. J, Huang R. B, Zheng L. S, Separation and Identification of Perchlorinated Polycyclic Aromatic Hydrocarbons and Fullerenes (C_{60} , C_{70}) by Coupling

- High-performance Liquid Chromatography with Ultraviolet Absorption Spectroscopy and Atmospheric Pressure Chemical Ionization Mass Spectrometry. *J. Chromatogr. A* 2001; 932(1-2): 43–53.
- [49] Weng Q. H, He Q, Sun, D, Hu. Y, Xie S. Y, Lu X, Huang R. B, Zheng L. S, Separation and Characterization of $C_{70}(C_{14}H_{10})$ and $C_{70}(C_5H_6)$ from an Acetylene–Benzene–Oxygen Flame. *J. Phys. Chem. C* 2011; 115(22): 11016-11022.
- [50] Wu X.Z, Yao Y. R, Chen M. M, H. R, Xiao J, Xu Y. Y, Lin M. S, Abella L, Tian C. B, Gao C. L, Zhang Q, Xie S. Y, Huang R. Y, Zheng L. S, Formation of Curvature Subunit of Carbon in Combustion. *J. Am. Chem. Soc.* 2016; 138 (30): 9629–9633.
- [51] Gao C. L, Abella L, Tan Y.-Z, Wu X.-Z, Rodríguez-Forteza A, Poblet J. M, et al. Capturing the Fused-Pentagon C_{74} by Stepwise Chlorination. *Inorg. Chem.* 2016; 55(14): 6861–5.
- [52] Kemnitz E, Troyanov S. I. Chlorides of Isomeric C_{78} Fullerenes: $C_{78}(1)Cl_{30}$, $C_{78}(2)Cl_{30}$, and $C_{78}(2)Cl_{18}$. *Mendeleev Commun.* 2010; 20(2): 74–6.
- [53] Troyanov S. I, Tamm N. B, Chen C, Yang S, Kemnitz E. Synthesis and Structure of a Highly Chlorinated C_{78} : $C_{78}(2)Cl_{30}$. *Z. Anorg. Allg. Chem.* 2009; 635(12): 1783–6.
- [54] Wang Y, Díaz-Tendero S, Alcamí M, Martín F. Relative Stability of Empty Exohedral Fullerenes: π Delocalization versus Strain and Steric Hindrance. *J. Am. Chem. Soc.* 2017; 139(4): 1609–17.
- [55] Khan S. I, Oliver A. M, Paddon-Row M. N, Rubin Y. Synthesis of a Rigid “ball-and-Chain” donor-Acceptor System through Diels-Alder Functionalization of Buckminsterfullerene

- (C₆₀). *J. Am. Chem. Soc.* 1993; 115(11): 4919–20.
- [56] Rubin Y, Khan S, Freedberg D. I, Yeretzyan C. Synthesis and X-Ray Structure of a Diels-Alder Adduct of Fullerene C₆₀. *J. Am. Chem. Soc.* 1993; 115(1): 344–5.
- [57] Simonyan A, Gitsov I. Linear-Dendritic Supramolecular Complexes as Nanoscale Reaction Vessels for “Green” Chemistry. Diels–Alder Reactions between Fullerene C₆₀ and Polycyclic Aromatic Hydrocarbons in Aqueous Medium. *Langmuir* 2008; 24(20): 11431–41.
- [58] Cui C.-X, Liu Y.-J. A DFT Study on Diels-Alder Cycloadditions of Trans -1,3-Butadiene to C₆₀ and C₇₀. *J. Phys. Org. Chem.* 2015; 28(4): 281–9.
- [59] Osuna S, Houk K. N. Cycloaddition Reactions of Butadiene and 1,3-Dipoles to Curved Arenes, Fullerenes, and Nanotubes: Theoretical Evaluation of the Role of Distortion Energies on Activation Barriers. *Chem. Eur. J.* 2009; 15 (47): 13219–31.
- [60] Osuna S, Swart M, Campanera J. M, Poblet J. M, Solà M. Chemical Reactivity of D_{3h} C₇₈ (Metallo)Fullerene: Regioselectivity Changes Induced by Sc₃N Encapsulation. *J. Am. Chem. Soc.* 2008; 130 (19): 6206–14.
- [61] Osuna S, Valencia R, Rodríguez-Forteza A, Swart M, Solà M, Poblet J. M. Full Exploration of the Diels-Alder Cycloaddition on Metallofullerenes M₃N@C₈₀ (M=Sc, Lu, Gd): The D_{5h} versus I_h Isomer and the Influence of the Metal Cluster. *Chem. Eur. J.* 2012; 18 (29): 8944–56.
- [62] Woodward R. B, Hoffmann R. The Conservation of Orbital Symmetry. *Angew. Chem. Int.*

Ed. Engl. 1969; 8(11): 781–853.

- [63] Fukui K, Yonezawa T, Shingu H. A Molecular Orbital Theory of Reactivity in Aromatic Hydrocarbons. *J. Chem. Phys.* 1952; 20(4): 722–5.
- [64] Fukui K. Recognition of Stereochemical Paths by Orbital Interaction. *Acc. Chem. Res.* 1971; 4(2): 57–64.
- [65] Fernández I, Solà M, Bickelhaupt F. M. Why Do Cycloaddition Reactions Involving C₆₀ Prefer [6,6] over [5,6] Bonds? *Chem. Eur. J.* 2013; 19(23): 7416–22.
- [66] Garcia-Borràs M, Osuna S, Luis J. M, Swart M, Solà M. The Role of Aromaticity in Determining the Molecular Structure and Reactivity of (Endohedral Metallo) fullerenes. *Chem. Soc. Rev.* 2014; 43(14): 5089-105.
- [67] Garcia-Borràs M, Osuna S, Swart M, Luis J. M, Solà M. Maximum Aromaticity as a Guiding Principle for the Most Suitable Hosting Cages in Endohedral Metallofullerenes. *Angew. Chem. Int. Ed.* 2013; 52(35): 9275–8.
- [68] Wang Y, Díaz-Tendero S, Martín F, Alcamí M. Key Structural Motifs To Predict the Cage Topology in Endohedral Metallofullerenes. *J. Am. Chem. Soc.* 2016; 138(5): 1551–60.
- [69] Wang Y, Díaz-Tendero S, Alcamí M, Martín F. Cage Connectivity and Frontier π Orbitals Govern the Relative Stability of Charged Fullerene Isomers. *Nat. Chem.* 2015; 7: 927–34.
- [70] Rodríguez-Fortea A, Alegret N, Balch A. L, Poblet J. M. The Maximum Pentagon Separation Rule Provides a Guideline for the Structures of Endohedral Metallofullerenes. *Nat. Chem.* 2010; 2 (11): 955–61.

[71] Rodríguez-Fortea A, Balch A. L, Poblet J. M. Endohedral Metallofullerenes: A Unique Host–guest Association. *Chem. Soc. Rev.* 2011; 40 (7): 3551-63.

[72] Alegret N, Abella L, Azmani K, Rodríguez-Fortea A, Poblet J. M. Different Factors Govern Chlorination and Encapsulation in Fullerenes: The Case of C₆₆. *Inorg. Chem.* 2015; 54 (15): 7562–70.